Int J Adv Manuf Technol (2017) 91:1631–1641
DOI 10.1007/s00170-016-9840-5

ORIGINAL ARTICLE

Adaptive MRAC-based direct torque control with SVM for sensorless induction motor using adaptive observer

Abdelkarim Ammar[1] · **Abdelhamid Benakcha**[1] · **Amor Bourek**[1]

Received: 4 August 2016 / Accepted: 25 November 2016 / Published online: 15 December 2016

Abstract This paper presents an improved direct torque control (DTC) method for induction motor (IM) drive. The main drawback of the conventional DTC is the use of hysteresis comparators which leads to high torque and flux ripples. The improvement in this paper includes using the space vector modulation to preserve a constant switching frequency and to reduce totally flux and torque ripples. Besides, the torque and stator flux regulation will be done based on model reference adaptive control (MRAC) strategy to ensure a robust control against external disturbance and less sensitivity from machine parameter variation unlike the conventional proportional-integral (PI) controllers. Furthermore, a design of an adaptive observer based on Lyapunov stability is presented for speed/flux and load torque estimation. The observer can improve the control performances and decrease the cost and increase reliability of the global control system by reducing the number of sensors. The proposed strategy will be examined under simulation tests using Matlab/Simulink and experimental implementation with real-time interface (RTI) based on dSpace 1104 board.

Keywords Induction motor · Direct torque control (DTC) · Space vector modulation (SVM) · Model reference adaptive control (MRAC) · Adaptive observer · dS 1104

✉ Abdelkarim Ammar
ammar.abdelkarim@yahoo.fr

[1] LGEB Laboratory, Electrical Engineering Department, Biskra University, Biskra, Algeria

1 Introduction

The direct torque control was proposed to ensure high-efficiency decoupled control of stator flux and electromagnetic torque. Unlike the field-oriented control (FOC), direct torque control (DTC) has more advantages like simple scheme, fast response, and less dependence on machine parameters. Moreover, it does not require coordinate transformation or current regulation loop. The control of stator flux and torque is based on hysteresis controllers and switching table to select an appropriate voltage vector of the inverter [1, 2]. However, the main problems of this method are the high level of torque and flux ripples and the variable switching frequency. Consequently, they lead to an acoustical and more control difficulty in low-speed region which will degrade the performance of the control algorithm [3].

Recently, different methods were proposed to minimize these drawbacks. The multilevel converters can provide low torque and stator flux ripples [4]. However, they increase the number of power switches which leads to a high cost and reduced the efficiency of the control system. The model predictive control (MPC) approach has the ability to determine a suitable voltage vector choice which can reduce the ripples [5]. However, the high complexity of the control law makes the main disadvantage to realize this strategy. The space vector modulation (SVM) strategy is also discussed in literature. It replaces the switching table by a voltage modulator for the voltage vector selection with maintaining a constant switching frequency. The first DTC based on SVM was introduced by [6]. The SVM-DTC can take various structures. Firstly, the closed-loop torque control uses a proportional-integral (PI) controller to adjust the changes of motor's torque in order to produce an appropriate voltage vector [7, 8]. The second method which becomes our interest in this paper is known by the stator-flux-oriented control (SFOC). This technique

uses two (PI) controllers instead of hysteresis controllers to generate direct and quadrature voltage components and achieve a decoupled control [9, 10].

However, the use of PI controllers requires the knowledge of the exact model of the controlled system. Besides, the selection of controller gains is not easy. Mostly, the gain values which are obtained by an analytical method or by simulation do not work well in practice. Usually, they adjusted by trial and error approximation. Moreover, the PI controllers have limited performances, especially while the presence of disturbances and uncertainties and parameter variation. As a result, the dynamic and stability of the system will be affected. Generally, machine parameter identification is done by experimental tests, so the measurement errors cannot be avoided. In addition, the parameters can be influenced by the environment condition (i.e., the resistance varies with temperature or the inductance with saturation).

Several robust control strategies have been presented to overcome these drawbacks, such as nonlinear sliding mode control (SMC), input-output feedback linearization (IOFL), and artificial intelligent techniques [10–13]. The variable structure control (VSC) has been combined with SVM-DTC by Lascu in [14]. This combination can achieve a robust control, but the disagreeable chattering phenomenon of the conventional SMC causes an infinite commutation which can excite high harmonics. The IOFL also has been presented with SVM-DTC in [15]. This strategy can provide decoupled control without chattering; however, the classical feedback linearization has a non-robust dynamic in the presence of uncertainties. In [10], a fuzzy logic-based SVM-DTC has been presented. However, the intelligent controllers can be very complex and need powerful calculation processes especially in real-time implementation.

The adaptive control theory takes an important part in modern control systems. It can work against various disturbances while the control system is running. The adaptive control has shown an apparent efficiency and a robust performance even without the exact knowledge of the system parameters [16, 17]. The model reference adaptive control (MRAC) strategy uses an adjustable controller and adjusting mechanism. Unlike the fixed-gain PI controller, MRAC is used to be more effective and handle the unknown parameter variation and external changes. It is based on dual-loop regulator, a normal feedback loop, and parameter-tuning loop. The parameters will be adjusted based on the errors between the reference model and the state plant in order to make a desired response which has been determined by the reference model [17, 18]. The combination of the adaptive control and SVM-DTC control scheme has been proposed in [19] for speed regulation only. In this paper, an implementation of MRAC controllers is presented in the entire of the control scheme to replace the conventional PI controllers for flux, torque decoupled control, and the outer speed regulation loop.

Over and above, this paper presents also a design of an observer to reduce the number of sensors which minimizes the cost of the control system of installation and cabling and improves system reliability [3, 20]. Many considerable researches have been proposed for electrical drives such as model reference adaptive system [21], sliding mode observers [8], and Kalman filter [3]. This work presents an adaptive observer based on Lyapunov theory to estimate stator flux, rotor speed, and load torque. The stator phase current and the flux will be considered as state variables, where the rotor speed is taken as an adaptive quantity [22, 23].

This paper presents a modified direct torque control of induction motor drive bases on the insertion of adaptive MRAC controllers in SVM-DTC algorithm. Furthermore, a design of stator flux adaptive observer is used for stator flux, speed, and load torque reconstruction. The proposed control scheme is examined by simulation and experimental implementation using Matlab/Simulink with real-time interface based on dSpace 1104 board. The simulation results and the experimental validation show that the combining of these techniques maintains good dynamic control with small ripples and accurate estimation in different operation conditions.

2 SVM-based direct torque control

2.1 Model dedicated for control of induction motor

The model equations of induction motor will be defined in the stationary frame reference as follows. The state variables are the stator phase currents and the stator flux:

$$\begin{cases} \frac{di_{s\alpha}}{dt} = -\left(\frac{R_s}{\sigma L_s} + \frac{R_r}{\sigma L_r}\right) i_{s\alpha} - \omega_r i_{s\beta} + \frac{R_s}{\sigma L_s L_r}\psi_{s\alpha} + \frac{\omega_r}{\sigma L_r}\psi_{s\beta} + \frac{1}{\sigma L_s} u_{s\alpha} \\ \frac{di_{s\beta}}{dt} = -\left(\frac{R_s}{\sigma L_s} + \frac{R_r}{\sigma L_r}\right) i_{s\beta} + \omega_r i_{s\alpha} + \frac{R_s}{\sigma L_s L_r}\psi_{s\beta} - \frac{\omega_r}{\sigma L_r}\psi_{s\alpha} + \frac{1}{\sigma L_s} u_{s\beta} \\ \frac{d\psi_{s\alpha}}{dt} = u_{s\alpha} - R_s i_{s\alpha} \\ \frac{d\psi_{s\beta}}{dt} = u_{s\beta} - R_s i_{s\beta} \end{cases} \quad (1)$$

where $i_{s\alpha}, i_{s\beta}$ are stator current components; $\psi_{s\alpha}, \psi_{s\beta}$ are stator flux components; R_s, R_r are stator and rotor resistance, respectively; L_s, L_r are stator and rotor inductance, respectively; $\sigma = 1 - \frac{M_{sr}}{L_s L_r}$ is Blondel's coefficient; and M_{sr} is the mutual stator-rotor inductance.

The electromagnetic torque can be expressed by the following:

$$T_e = p\left(\psi_{s\alpha} i_{s\beta} - \psi_{s\beta} i_{s\alpha}\right) \quad (2)$$

2.2 SFOC control strategy

The SVM-DTC control strategy is expressed in stator-flux-oriented coordinates (SFOC). The orientation makes a decoupling between flux and torque where the stator flux vector becomes aligned with the *d*-axis. It is well known that the *q*-axis is the magnetizing axis and the *q*-axis is the torque axis [10]. The model in synchronous frame can be expressed as follows:

$$\psi_{sd} = \psi_s \; ; \psi_{sq} = 0 \tag{3}$$

The voltage model can be written as follows:

$$v_{sd} = R_s i_{sd} + \frac{d\psi_s}{dt} \tag{4}$$

$$v_{sq} = R_s i_{sq} + \omega_s \psi_s \tag{5}$$

The electromagnetic torque is as follows:

$$T_e = p\psi_s i_{sq} \tag{6}$$

The voltage model expresses that the stator flux and torque are related with *d*-*q* components; Eq. (5) can be written as follows:

$$v_{sq} = \frac{R_s T_e}{p\psi_s} + \omega_s \psi_s \tag{7}$$

2.3 Space vector modulation

The produced reference voltages by the control law will be coordinate transformed; after that, the SVM unit modulates them to generate the inverter's command states. The switching frequency of the space vector modulation is constant; as a result, it can reduce considerably the torque and flux ripples. The principle of SVM method is to predict the voltage vector and calculate it based on each of the three adjacent vectors in each sector. The application time for each vector can be obtained by vector calculations, and the rest of the time period will be spent by applying the null vector [6, 8]. The space vector for a two-level inverter is shown in Fig. 1.

$$T_1 = \frac{T_z}{2U_{dc}}\left(\sqrt{6}V_{s\beta\text{ref}} - \sqrt{2}V_{s\alpha\text{ref}}\right) \tag{8}$$

$$T_2 = \sqrt{2}\frac{T_z}{U_{dc}}V_{s\alpha\text{ref}} \tag{9}$$

T_1, T_2 are the corresponding vector durations; T_z is the sampling time; $V_{s\alpha}, V_{s\beta}$ are reference stator voltage components in stationary frame; and U_{dc} is DC voltage.

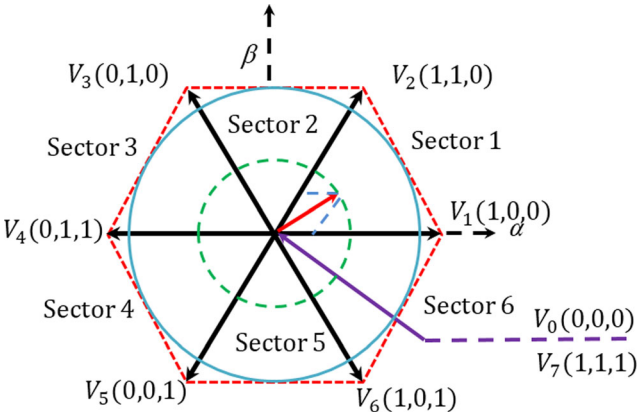

Fig. 1 Diagram of voltage space vector

3 Control design using model reference adaptive controller

The aforementioned algorithm is based generally on two decoupled PI controllers which receive the stator flux and torque tracking errors as inputs and generate the *d*-*q* component voltage in a synchronous reference frame [10]. In this paper, the classical PI controllers will be replaced by adaptive MRAC controllers for this operation.

3.1 MRAC flux and electromagnetic torque control

The MRAC control law is designed in order to generate the reference voltages and to update the primary controller law parameters. As a result, the system responses follow their desired references [24].

The model reference adaptive control block diagram is illustrated in Fig. 2. As shown, it is composed of three parts: reference model which gives the desired response of the adaptive control, then the controller which contains the adjustable parameters, and finally the adaptation law which is used for tuning controller parameters. This control is based on comparing the

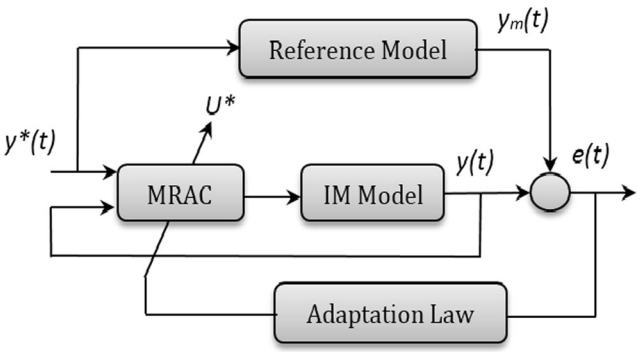

Fig. 2 Diagram of MRAC

system output with the reference model output. An error signal $e(t)$ will be produced. The output signal of the adaptation mechanism law is used for adjusting parameters.

Our studied system can be represented based on a first-order linear plant approximation by:

$$y(t) = -ax(t) + bu(t) \tag{10}$$

where $x(t)$ is the plant state (the output of the system), in our case, the system outputs are represented by the stator flux and the electromagnetic torque; $u(t)$ is the input (control signal); and a and b are the state plant parameters.

The reference model can be defined as:

$$\dot{y}_m(t) = -a_m x_m(t) + b_m r(t) \tag{11}$$

where $x_m(t)$ is the output of the reference model; a_m and b_m are the reference model parameters; and $r(t)$ is an external reference signal. The tracking error $e(t)$ can be defined as:

$$e(t) = x_m(t) - x(t) \tag{12}$$

The adaptive control law has been designed based on the minimal control synthesis (MCS) algorithm which is presented in [25]. The MCS algorithm is a development of MRAC and has a similarity which is based on the hyperstability theory of Popov.

The control law is generated by multiplying the state variable and the reference signal $r(t)$ with the adaptive control gains K and K_r, as given below:

$$u(t) = K(t)x(t) + K_r(t)r(t) \tag{13}$$

where $K(t)$ and $K_r(t)$ are the feedback and the feedforward adaptive gains, respectively. The values of the adaptive gains $K(t)$ and $K_r(t)$can be defined according to the following equations [16, 25]:

$$\begin{cases} K(t) = \alpha \int_0^t y_e.x^T(t)dt + \beta.y_e.x^T(t) \\ K_r(t) = \alpha \int_0^t y_e.r(t)dt + \beta.y_e.r(t) \end{cases} \tag{14}$$

where:

$$\begin{cases} r(t) = \left(\psi_s^*, T_e^*\right) \\ x(t) = (\psi_s, T_e) \end{cases} \tag{15}$$

α and β are adaptive control weightings. The initial conditions are usually set to zero [25].

The output error is obtained as:

$$y_e = C_e e(t) \tag{16}$$

C_e should be chosen as much as the feedforward part is stable.

The controller outputs are the reference voltage components in d-q frame which can defined as:

$$\begin{cases} V_{sd} = K_u(t)\psi_s^* + K_p(t)\psi_s \\ V_{sq} = K_u(t)T_e^* + K_p(t)T_e \end{cases} \tag{17}$$

In addition, the reference torque T_e^* is generated by speed-control loop. The speed MRAC control law is given by:

$$T_e = K\omega^* + K_r\omega \tag{18}$$

The tracking error can be defined by:

$$e(t) = \omega^* - \omega \tag{19}$$

4 Adaptive flux observer design

By considering the stator phase current and the stator flux as state variables, the induction motor model which is given in Eq. (1) can be formed as:

$$\frac{d}{dt}\begin{bmatrix} i_s \\ \psi_s \end{bmatrix} = \begin{bmatrix} A_{11} & A_{12} \\ A_{21} & A_{21} \end{bmatrix}\begin{bmatrix} i_s \\ \psi_s \end{bmatrix} + \begin{bmatrix} B_1 \\ B_2 \end{bmatrix}[V_s] = Ax + Bu_s \tag{20}$$

where:

$$i_s = Cx \tag{21}$$

Vs is the system input (the voltage vector).

$$V_s = \begin{bmatrix} V_{s\alpha} & V_{s\beta} \end{bmatrix}^T$$

$$A_{11} = -\left(\frac{1}{\sigma T_s} + \frac{1}{\sigma T_r}\right)I - \omega_r J; \quad I = \begin{bmatrix} 1 & 0 \\ 0 & 1 \end{bmatrix}$$
$$A_{12} = \frac{1}{\sigma L_s T_s} I + \frac{\omega_r}{\sigma T_s} J, \quad J = \begin{bmatrix} 0 & -1 \\ 1 & 0 \end{bmatrix}$$
$$A_{21} = -R_s I; \quad A_{22} = 0$$
$$B_1 = \frac{1}{\sigma L_s} I; \quad B_2 = I$$
$$C = [I \quad 0]$$

Then, the state observer will be described as follows [10, 23, 26]:

$$\frac{d\hat{x}}{dt} = \hat{A}\hat{x} + Bu_s + G\left(\hat{i}_s - i_s\right) \tag{22}$$

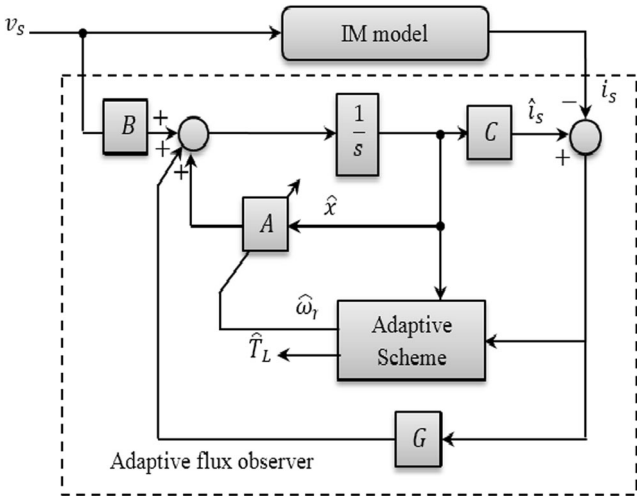

Fig. 3 Block diagram of speed adaptive flux observer

G is the observer gain matrix, and the estimated values are marked with the sign of a hat (^).

By subtracting Eq. (22) from Eq. (20), the estimation error is defined as follows:

$$\frac{de_i}{dt} = (A + GC)e_i + \Delta Ax \tag{23}$$

where:

$$e_i = x - x$$

$$\Delta A = A - \hat{A} = \begin{bmatrix} -\Delta\omega_r J & \frac{\Delta\omega_r}{\sigma L_s} J \\ 0 & 0 \end{bmatrix}$$

$$\Delta\omega_r = \omega_r - \hat{\omega}_r$$

The Lyapunov function *V* will be defined to ensure the stability.

$$V = e^T e + \frac{\left(\omega_r - \hat{\omega}_r\right)^2}{\lambda} \tag{24}$$

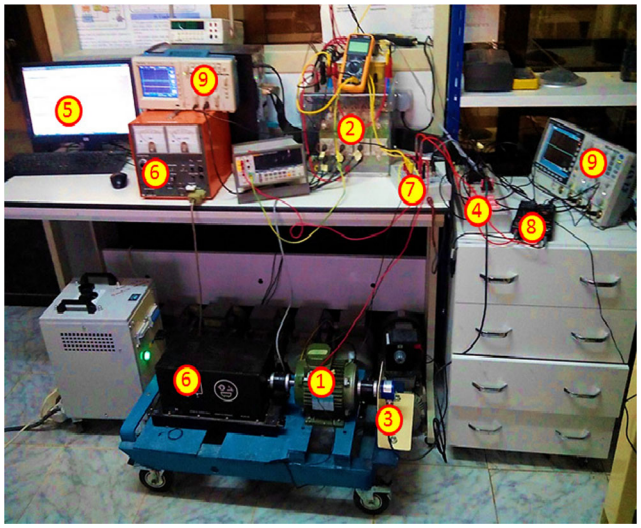

Fig. 5 Experimental setup

where λ is a positive constant.

The time derivative of *V* is given by:

$$\dot{V} = e^T\left[(A + GC)^T + (A + GC)\right]e + \hat{x}^T \Delta A^T e + e^T \Delta A \hat{x} - 2\frac{\Delta\omega_r}{\lambda}\frac{\Delta\hat{\omega}_r}{dt} \tag{25}$$

The derivative of the Lyapunov function must be negative to guarantee the stability. The gain matrix *G* must be chosen as much as the first term of Eq. (25) is negative semi-definite [26].

The adaptive scheme for speed estimation can be determined from the second and third terms.

$$\hat{\omega}_r = K_\omega \int \left[e_{s\alpha}\left(\frac{\hat{\psi}_{s\beta}}{\sigma L_s} - \hat{i}_{s\beta}\right) - e_{s\beta}\left(\frac{\hat{\psi}_{s\alpha}}{\sigma L_s} - \hat{i}_{s\alpha}\right)\right] \tag{26}$$

When the load torque is unknown or variable, it is considered as a system uncertainty. In this paper, an enhanced model will be used in order to improve the response of the estimated speed and estimate the applied load torque on the induction motor without the need of

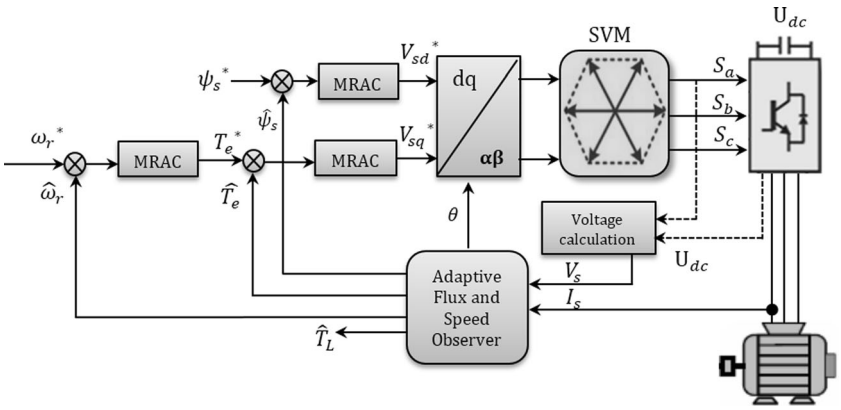

Fig. 4 Global diagram of sensorless adaptive MRAC SVM-DTC with adaptive observer

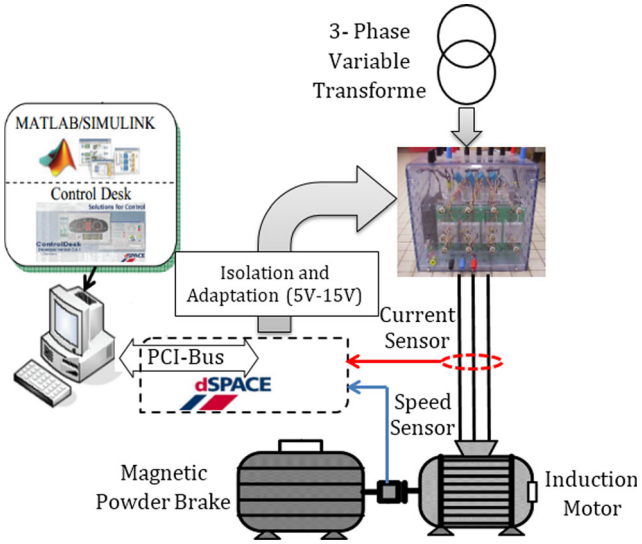

Fig. 6 Simplified setup scheme

any torque sensor and to improve the control performance by reducing the system uncertainty.

$$\begin{cases} \hat{\omega} = \dfrac{1}{J}\left(T_e - \hat{T}_L\right) \\ \dot{\hat{T}}_L = 0 \end{cases} \tag{27}$$

where $\hat{T}_L$ is the estimated load torque.

The friction coefficient will be neglected, and the load torque will be considered as constant. The speed adaptive scheme becomes

$$\omega_r = \frac{1}{J}\int \left(T_e - \hat{T}_L\right) + K_\omega \int \left[e_{s\alpha}\left(\frac{\hat{\psi}_{s\beta}}{\sigma L_s} - \hat{i}_{s\beta}\right) - e_{s\beta}\left(\frac{\hat{\psi}_{s\alpha}}{\sigma L_s} - \hat{i}_{s\alpha}\right)\right] \tag{28}$$

The load torque can be estimated as follows:

$$\hat{T}_L = -K_T \int \left[e_{s\alpha}\left(\frac{\hat{\psi}_{s\beta}}{\sigma L_s} - \hat{i}_{s\beta}\right) - e_{s\beta}\left(\frac{\hat{\psi}_{s\alpha}}{\sigma L_s} - \hat{i}_{s\alpha}\right)\right] \tag{29}$$

K_ω and K_T are arbitrary positive gains.

To ensure stability of the observer, the poles must be selected proportional to the induction machine poles. If we define the machine poles by s_{IM}, the observer poles will be defined by [23, 26]:

$$s_o = k_p s_{IM} \tag{30}$$

k_p is a factor ($k_p > 1$) which indicates that the observer is dynamically faster than the machine. Then, the gain matrix can be obtained by:

$$G = \begin{bmatrix} g_1 I & g_2 J \\ g_3 I & g_4 J \end{bmatrix} \tag{31}$$

where g_1, g_2, g_3, g_4 are the observer gains. They can be founded from motor parameters and motor speed.

The block diagram of the adaptive flux observer is shown in Fig. 3.

Figure 4 shows the global block diagram of the adaptive MRAC-based SVM-DTC with adaptive observer.

5 Simulation and experimental results

The described control theory above has been simulated by Matlab/Simulink software. The simulation results were obtained for a three-phase 1.1-kW squirrel-cage induction motor with characteristics given in "Appendix." The proposed control scheme has been verified also by the experimental

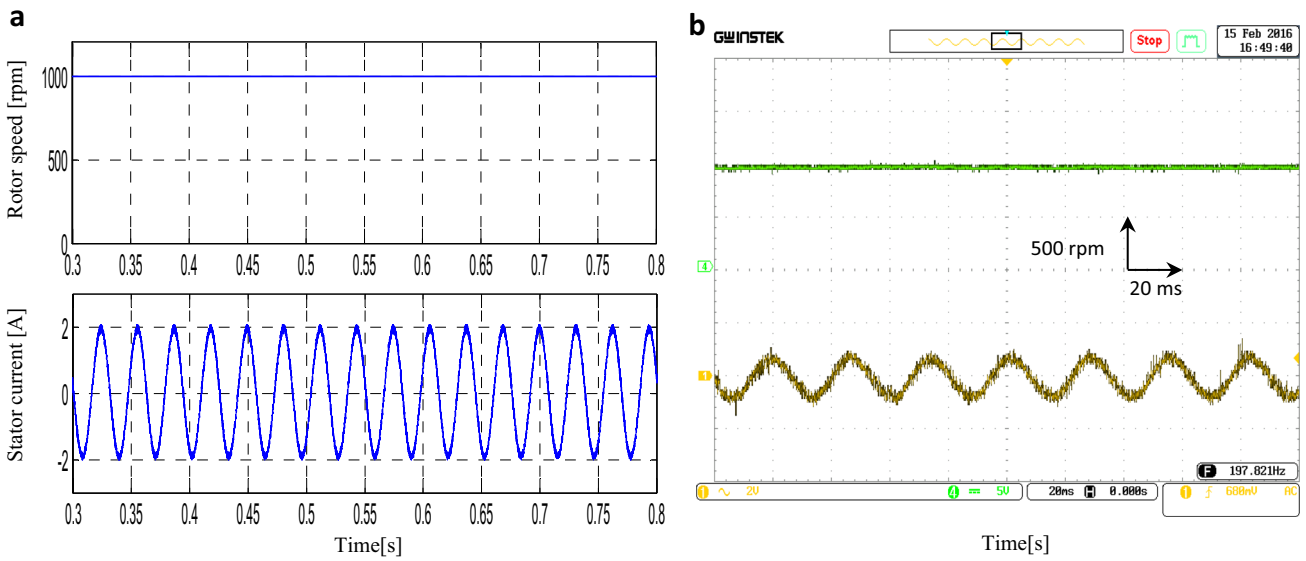

Fig. 7 Steady state: rotor speed [rpm], stator phase current [A]. **a** For simulation. **b** For experimental results

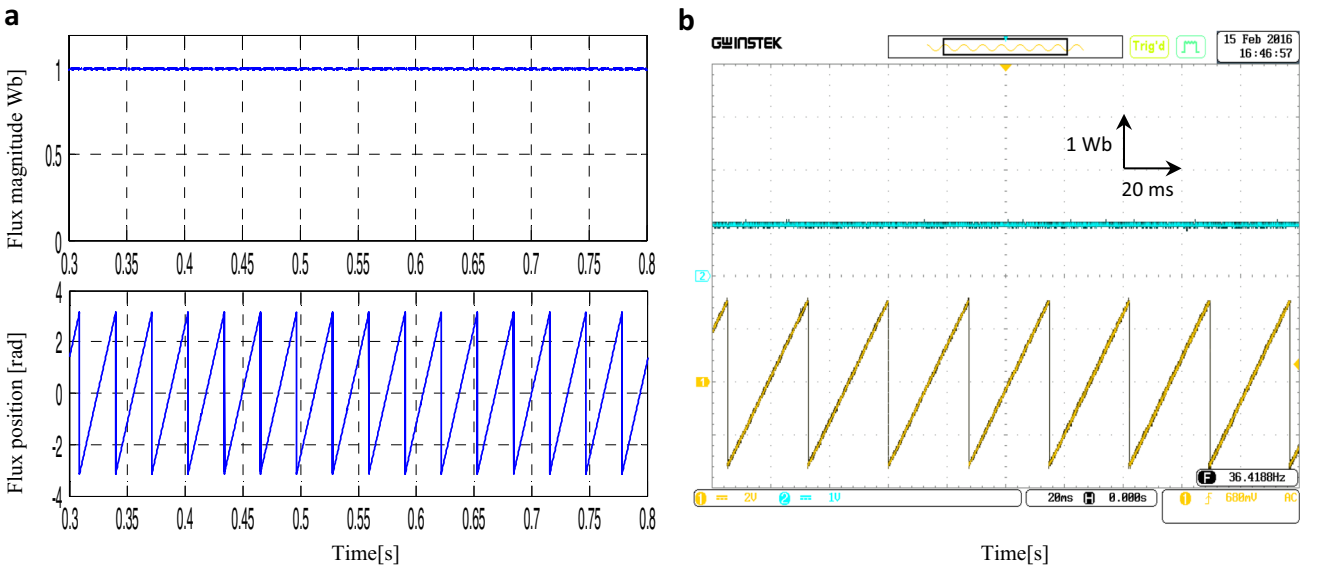

Fig. 8 Steady state: stator flux magnitude [Wb], flux angle [rad]. **a** For simulation. **b** For experimental results

implementation. The real-time control was done in the laboratory equipped with dSpace 1104 board. The implementation ground of the induction motor drive is essentially composed as shown in Fig. 5 of (1) a squirrel-cage induction motor (IM) 1.1 kW; (2) Semikron power converter composed of a rectifier and IGBT inverter; (3) speed sensor (incremental encoder), it will be used in order to check and compare the real speed with the estimated speed; (4) dSpace DS 1104 with (5) control desk software plugged in a personal computer; (6) magnetic powder brake with load control unit; (7) Hall-type current sensors; (8) voltage sensors; and (9) numerical oscilloscope.. In order to reduce the cost of global control system, the phase voltages will be estimated just from DC-bus voltage and inverter switching states (S_a, S_b, S_c) [8]. Figure 6 shows a simplified setup scheme.

The experimental results of sensorless SVM-DTC with adaptive MRAC controllers and adaptive observers have been obtained by using GW-INSTEK numerical oscilloscope which was linked with the real-time interface. The suitable choice of sampling frequency has an apparent influence on quality of signals (i.e., phase current and torque). The sampling frequency of dSpace 1104 can reach to 20 kHz. However, due to some limits and constraints imposed by the real-time implementation and control scheme complexity, we were obliged to choose a reducer value of sampling frequency which is 10 kHz.

The figures below show the simulation and experimental results of the sensorless control scheme in different operation modes of the IM drive, such as the following: steady state, speed reversing, load application, and low-speed test. In addition, the load torque estimation has been presented.

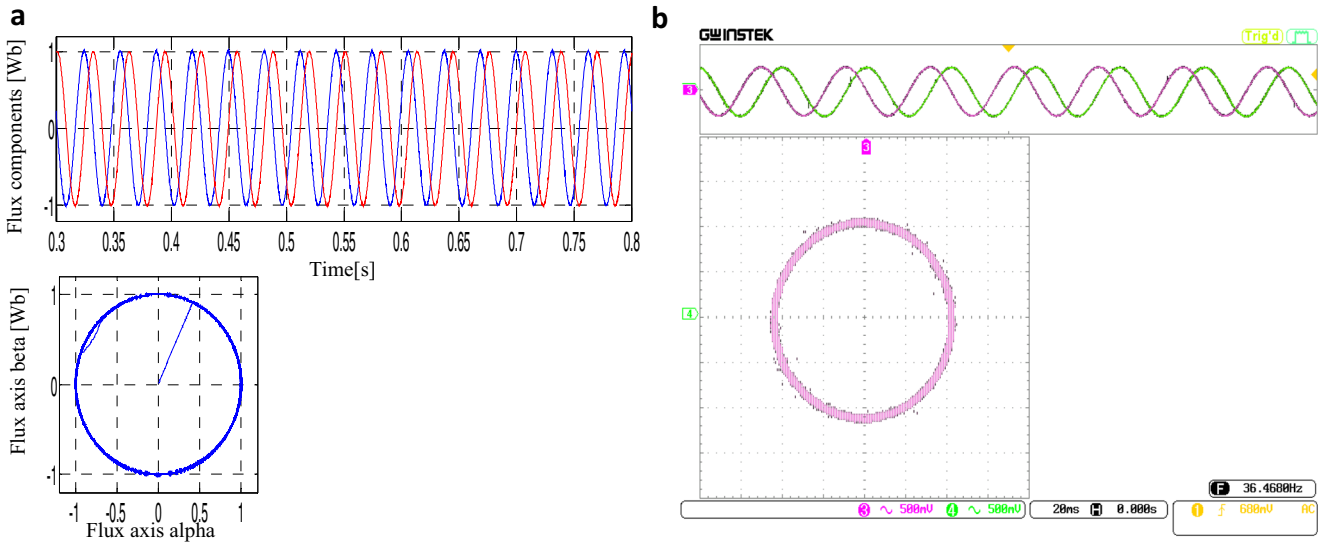

Fig. 9 Steady state: stator flux components [Wb], flux circular trajectory (α, β). **a** For simulation. **b** For experimental results

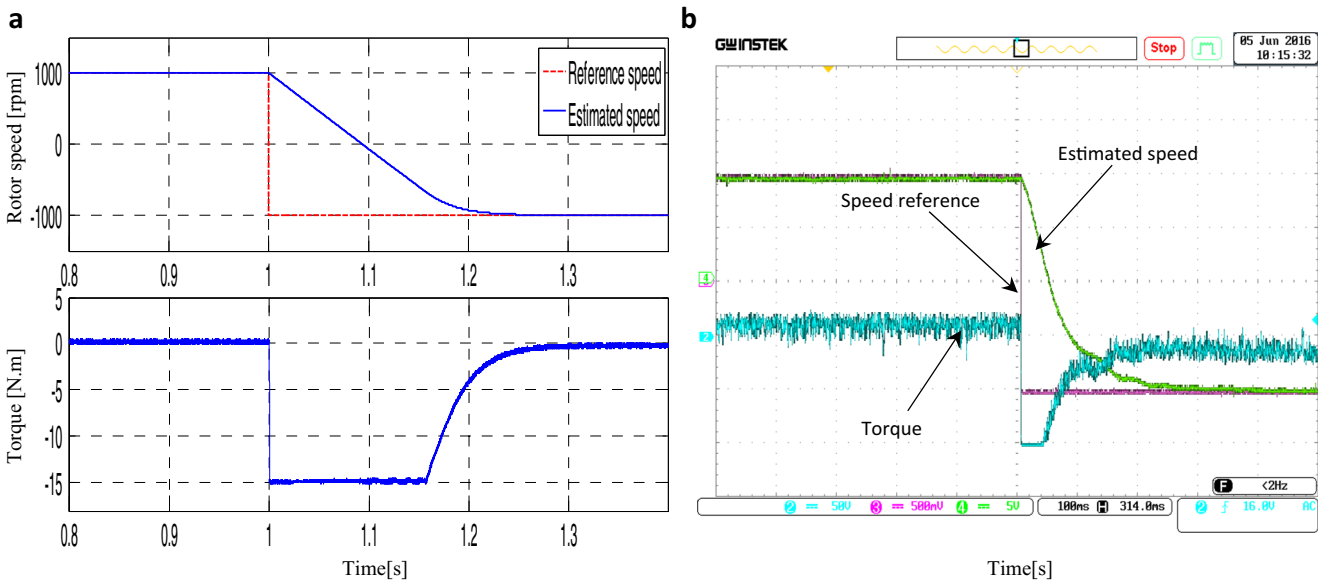

Fig. 10 Speed sense reversing: rotor speed [rpm], electromagnetic torque [N.m]. **a** For simulation. **b** For experimental results

Firstly, Fig. 7 presents the simulation and experimental results of steady state of the controlled motor without load application. This figure shows the rotor speed (1div = 500 rpm) and stator phase current i_{sa}. The rotor speed has good reference tracking (1000 rpm). Both simulation and experimental results show good sinusoid waveform and the reduced harmonics of the current as a result of applying SVM. Figure 8a, b illustrates the stator flux magnitude with its angle; the flux follows the reference value 1 Wb (1div = 1 Wb). In Fig. 9a, b, we can see the stator flux (α, β) axis components and trajectory. The simulation and the real implementation show low ripple level of the stator flux and good sinusoid waveform of flux components also. Next, in Figs. 10, 11, and 12, the speed sense reversing has been done. The simulation and experimental results that are shown in Fig. 10 illustrate the speed and electromagnetic torque while sense reversing. The sensorless control strategy has a good speed and torque dynamic during this operation. In addition, the torque shows reduced ripples. Figure 11 presents the estimated and real speeds; both speeds have a full superposition while the estimation error converges to zero which indicates to an accurate estimation. To confirm the satisfied performance of the flux observer, Fig. 12 shows the reversing of flux components and angle. This figure shows the robustness of the control algorithm while sense reversing. Then, Fig. 13 illustrates the load introduction of 5 N.m; the figure shows the electromagnetic torque (1div = 5 N.m) and current. The torque has fast responding to the load application and low ripples

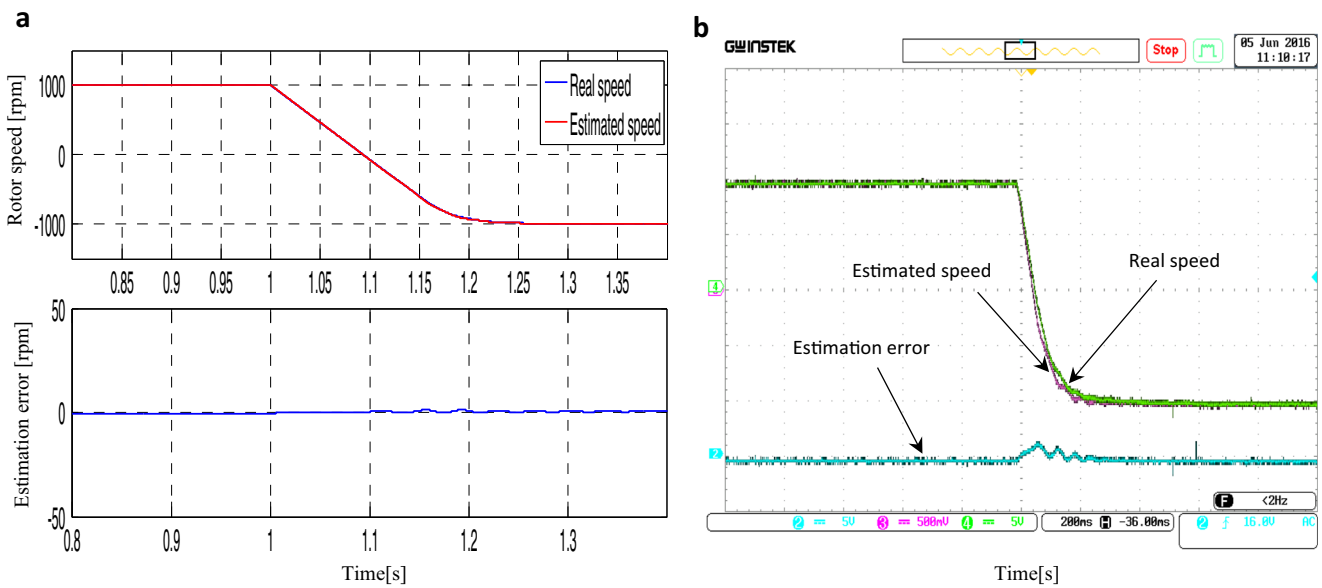

Fig. 11 Speed sense reversing: estimated and real speeds [rpm], estimation error [rpm]. **a** For simulation. **b** For experimental results

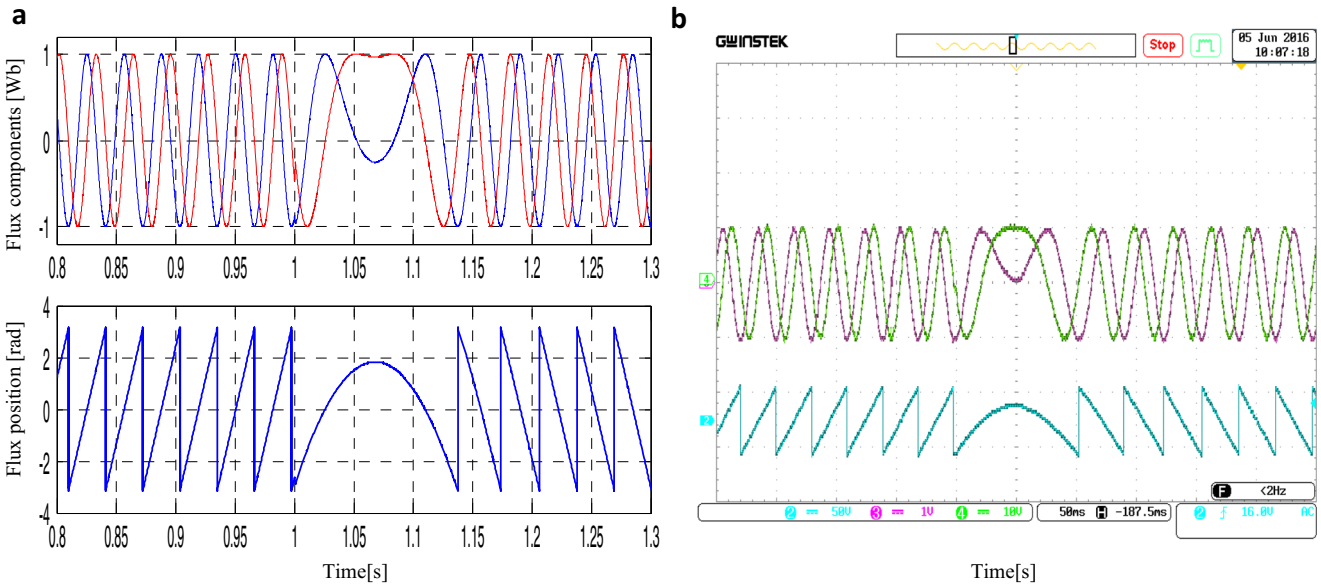

Fig. 12 Speed sense reversing: stator flux components [Wb], flux position [rad]. **a** For simulation. **b** For experimental results

while the current shows good waveform and low harmonics in both simulation and real-time implementation. The low-speed test is presented in Fig. 14; it shows from the top to the bottom: flux angle, estimated and real speeds, and estimation error with reference variation at very low speed values (50 and 200 rpm). The speed presents good reference tracking; the estimated speed follows the real one in a prefect superposition where the estimation error converges to zero. The flux angle has been added to indicate the variation of rotation frequency. These tests prove that the sensorless control technique kept its good performance and accurate estimation in low-speed conditions also. Finally, Fig. 15 shows the load torque estimation. The figure illustrates the applied load torque with the estimation error. We can see a good superposition between the estimated value and the real one. The error converges quickly to zero.

In general, the experimental results have validated the simulation results and gave a similar behavior in all tests. However, it is noticed that there is a small disagreement between them. This may be owing to many reasons: the limited sampling time of our processor, the ideality of simulation environment and the inaccuracies which exist in real-time implementation, the dead times of the inverter power switching signals, the offset of measurement instruments, and, in addition, the motor losses which are not taken into account in our system modeling.

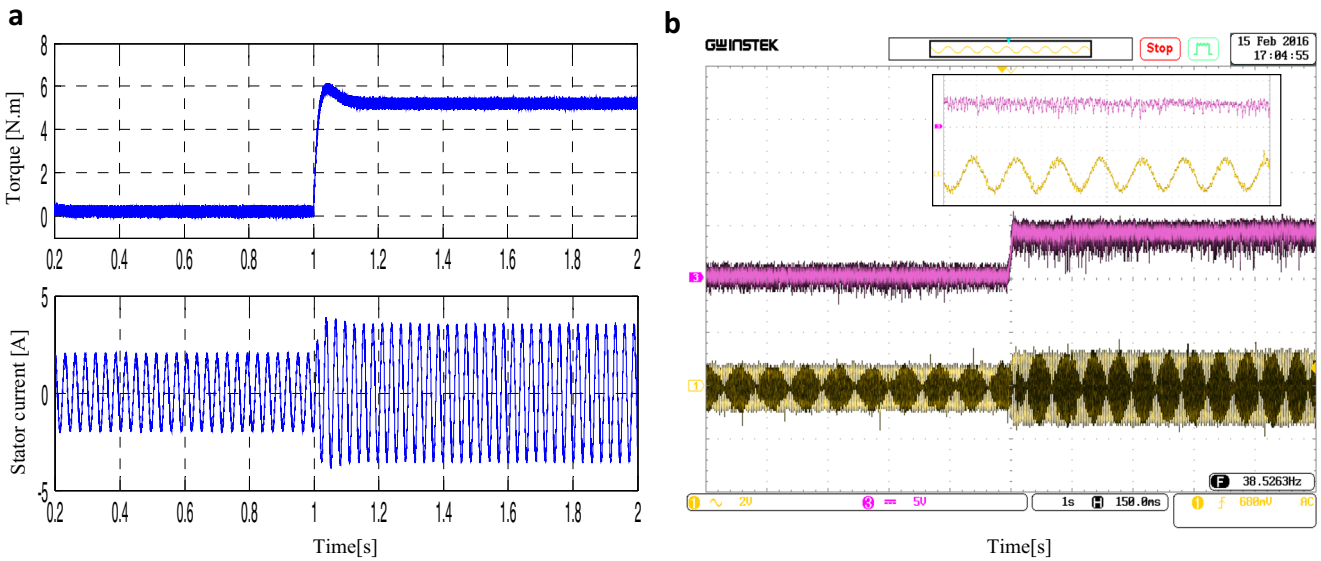

Fig. 13 Load application: electromagnetic torque [N.m], stator phase current [A]. **a** For simulation. **b** For experimental results

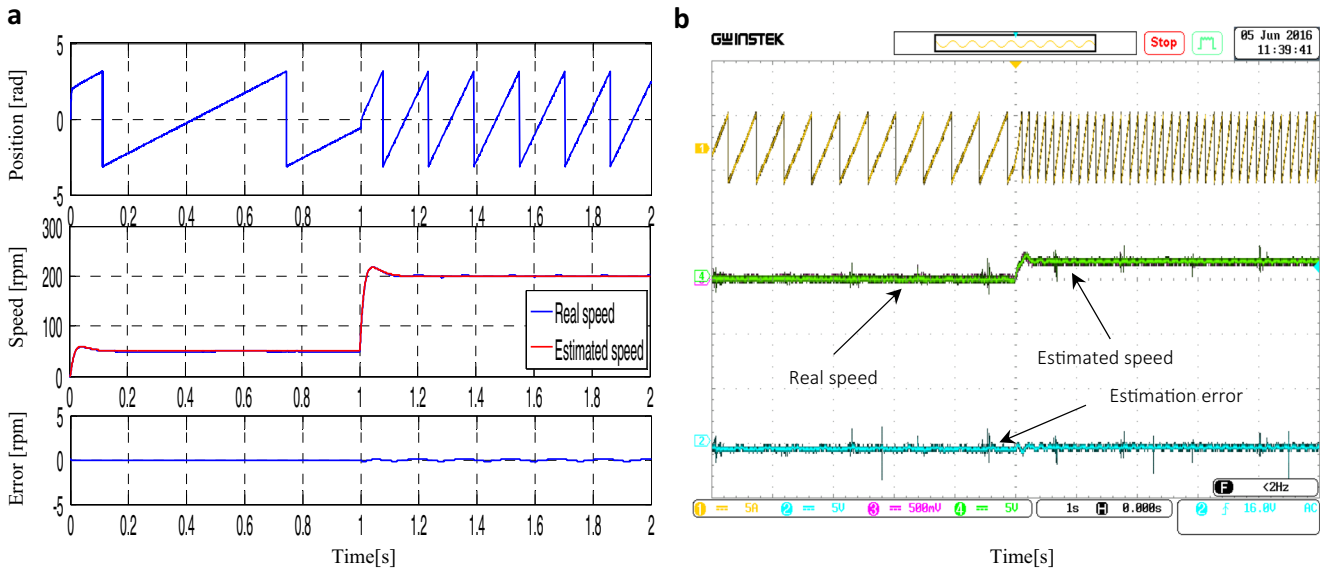

Fig. 14 Low-speed operation: flux position [rad], estimated and real speeds [rpm], estimation error [rpm]. **a** For simulation. **b** For experimental results

6 Conclusion

This paper presents a sensorless control strategy composed of stator field-oriented SVM-DTC based on model adaptive reference controllers (MRACs) combined with an adaptive observer for induction motor drive. The direct and quadrature reference voltages have been generated based on MRAC controllers in order to achieve a decoupled flux and torque control. The SVM preserves a low ripple and harmonic level. This combination can overcome different drawbacks belonging to PI-based DTC scheme. Furthermore, the control scheme has been incorporated with an observation strategy. An adaptive observer based on Lyapunov stability has been proposed to ensure an accurate speed and flux estimation and improve system reliability.

The effectiveness and performance of the sensorless strategy have been verified by simulation and real-time implementation. Different tests have been operated. The simulation and the experimental validation results have been presented. MRAC controllers have a fast, dynamic, good tracking and a robustness against parameter variation and external load disturbance; they can solve various PI problems. The control strategy maintains a reduced torque/flux ripple and good performances during low-speed operation. Besides, the adaptive observer has shown good accuracy and acceptable error level in speed/flux and load estimation, robustness in different operation condition (i.e., sense reverse, low-speed region).

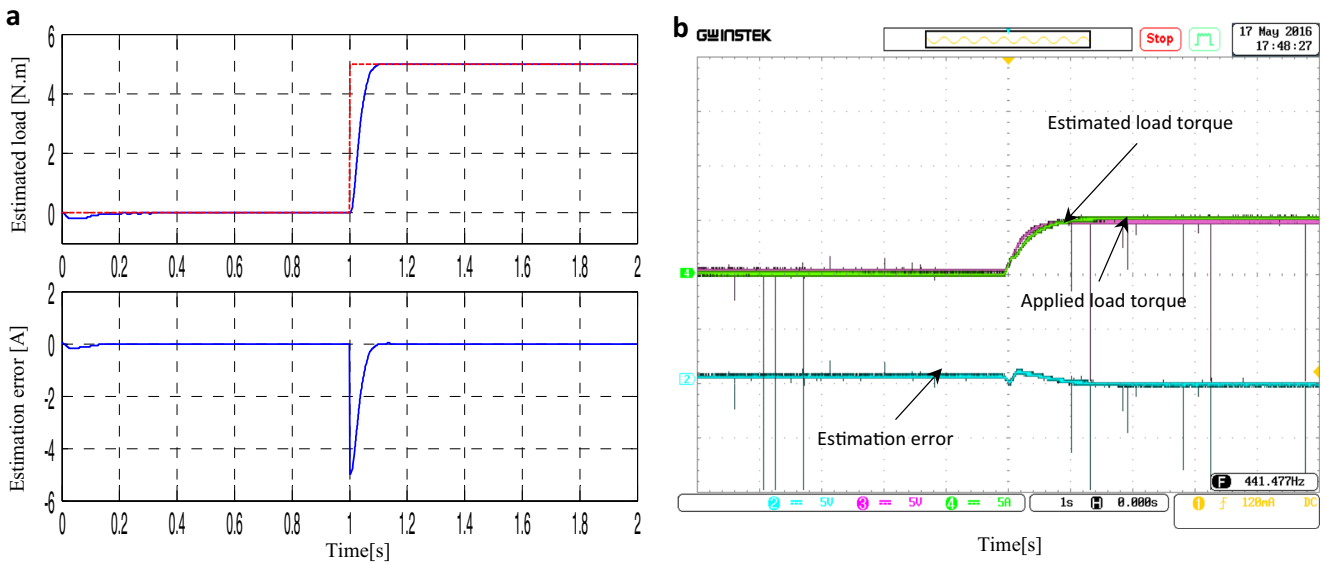

Fig. 15 Load torque estimation: applied and estimated load torque [N.m], estimation error [N.m]. **a** For simulation. **b** For experimental results

Generally, SVM-DTC is a good solution to improve the classical DTC performances; the insertion of robust adaptive controllers and observers gets more high performances for induction motor electrical drive.

Appendix

The parameters of the three-phase induction motor, employed for simulation and real implementation, in SI units are the following:

1.1 kW, 50 Hz, $p = 2$, $R_s = 6.75\ \Omega$, $R_r = 6.21\ \Omega$, $L_s = L_r = 0.5192$ H, $M_{sr} = 0.4957$ H, $f_r = 0.002$ SI, $J = 0.01240\ \text{kg.m}^2$

Reference

1. Casadei D, Profumo F, Serra G, Tani A (2002) FOC and DTC: two viable schemes for induction motors torque control. IEEE Trans Power Electron 17:779–787. doi:10.1109/TPEL.2002.802183
2. Ren Y, Zhu ZQ (2015) Enhancement of steady-state performance in direct-torque-controlled dual three-phase permanent-magnet synchronous machine drives with modified switching table. IEEE Trans Ind Electron 62:3338–3350. doi:10.1109/TIE.2014.2376881
3. Alsofyani IM, Idris NRN (2016) Simple flux regulation for improving state estimation at very low and zero speed of a speed sensorless direct torque control of an induction motor. IEEE Trans Power Electron 31:3027–3035. doi:10.1109/TPEL.2015.2447731
4. VN N, Panda A, Singh SP (2016) A three-level fuzzy-2 DTC of induction motor drive using SVPWM. IEEE Trans Ind Electron 63: 1467–1479. doi:10.1109/TIE.2015.2504551
5. Mesloub H, Benchouia MT, Goléa A et al (2016) Predictive DTC schemes with PI regulator and particle swarm optimization for PMSM drive: comparative simulation and experimental study. Int J Adv Manuf Technol. doi:10.1007/s00170-016-8406-x
6. Habetler TG, Profumo F, Pastorelli M, Tolbert LM (1992) Direct torque control of induction machines using space vector modulation. Ind Appl IEEE Trans 28:1045–1053. doi:10.1109/28.158828
7. Rodriguez J, Pontt J, Silva C, et al. (2004) A novel direct torque control scheme for induction machines with space vector modulation. IEEE 35th annu power electron spec conf (IEEE Cat No04CH37551) 1392–1397. doi: 10.1109/PESC.2004.1355626
8. Ammar A, Bourek A, Benakcha A (2015) Modified load angle direct torque control for sensorless induction motor using sliding mode flux observer. In: 2015 4th int. conf. electr. eng. IEEE, pp 1–6
9. Lascu C, Boldea I, Blaabjerg F (2000) A modified direct torque control for induction motor sensorless drive. IEEE Trans Ind Appl 36:122–130. doi:10.1109/28.821806
10. Saberi H, Feyzi M, Sharifian MBB, Sabahi M (2014) Improved sensorless direct torque control method using adaptive flux observer. IET Power Electron 7:1675–1684. doi:10.1049/iet-pel.2013.0390
11. Fu X, Li S (2015) A novel neural network vector control technique for induction motor drive. IEEE Trans Energy Convers 30:1428–1437. doi:10.1109/TEC.2015.2436914
12. Stavropoulos P, Chantzis D, Doukas C, Papacharalampopoulos A (2013) Monitoring and control of manufacturing processes: a review. Procedia CIRP 8:421–425. doi:10.1016/j.procir.2013.06.127
13. Choi YS, Choi HH, Jung JW (2016) Feedback linearization direct torque control with reduced torque and flux ripples for IPMSM drives. IEEE Trans Power Electron 31:3728–3737. doi:10.1109/TPEL.2015.2460249
14. Lascu C, Trzynadlowski AM (2004) Combining the principles of sliding mode, direct torque control, and space-vector modulation in a high-performance sensorless AC drive. 40:170–177
15. Zhang Z, Tang R, Bai B, Xie D (2010) Novel direct torque control based on space vector modulation with adaptive stator flux observer for induction motors. IEEE Trans Magn 46:3133–3136. doi:10.1109/TMAG.2010.2051142
16. Astrom KJ, Wittenmar B (1994) Adaptive control, 2nd edn. Addison-Wesley Longman Publishing Co., Inc., Boston
17. Abdeddaim S, Betka A, Drid S, Becherif M (2014) Implementation of MRAC controller of a DFIG based variable speed grid connected wind turbine. Energy Convers Manag 79:281–288. doi:10.1016/j.enconman.2013.12.003
18. Wu G-Q, Wu S-N, Bai Y-G, Liu L (2013) Experimental studies on model reference adaptive control with integral action employing a rotary encoder and tachometer sensors. Sensors 13:4742–4759. doi:10.3390/s130404742
19. Belkacem S, Naceri F, Abdessemed R (2011) Improvement in DTC-SVM of AC drives using a new robust adaptive control algorithm. Int J Control Autom Syst 9:267–275. doi:10.1007/s12555-011-0208-1
20. Barambones O, Alkorta P (2014) Position control of the induction motor using an adaptive sliding-mode controller and observers. IEEE Trans Ind Electron 61:6556–6565. doi:10.1109/TIE.2014.2316239
21. Cirrincione M, Pucci M (2005) An MRAS-based sensorless high-performance induction motor drive with a predictive adaptive model. 52:532–551
22. Naifar O, Boukettaya G, Ouali A (2015) Global stabilization of an adaptive observer-based controller design applied to induction machine. Int J Adv Manuf Technol 81:423–432. doi:10.1007/s00170-015-7099-x
23. Yin Z, Zhang Y, Du C et al (2016) Research on anti-error performance of speed and flux estimation for induction motors based on robust adaptive state observer. IEEE Trans Ind Electron 63:3499–3510. doi:10.1109/TIE.2016.2524414
24. Guo L, Parsa L (2012) Model reference adaptive control of five-phase IPM motors based on neural network. IEEE Trans Ind Electron 59:1500–1508. doi:10.1109/TIE.2011.2163371
25. STOTEN DP, DI BERNARDO M (1996) Application of the minimal control synthesis algorithm to the control and synchronization of chaotic systems. Int J Control 65:925–938. doi:10.1080/00207179608921731
26. Maes J, Melkebeek JA (2000) Speed-sensorless direct torque control of induction motors using an adaptive flux observer. IEEE Trans Ind Appl 36:778–785. doi:10.1109/28.845053